

# MODELLING AND SIMULATION OF DYNAMIC UNILATERAL ELASTO-PLASTIC CONTACT OF COMPACT HARD BODIES

ZOFIA KOWALSKA

*Institute of Fundamental Technological Research PAS,  
Świętokrzyska 21, 00-049 Warsaw, Poland  
zkowal@ippt.gov.pl*

(Received 2 May 2002)

**Abstract:** The problems of modelling, simulation and analysis of vibro-impact motion of compact hard bodies are considered. In particular, dynamic elasto-plastic contact is simulated by using Johnson's analytical model of spherical bodies' contact. The results are compared with behaviour of the system with discrete linear-perfectly plastic model of contact.

**Keywords:** motion simulation, non-linear dynamics, vibro-impact systems

## *Notation*

- $Y$  – uniaxial yield stress,
- $\bar{p}_Y$  – limiting mean pressure on contact surface,
- $\vartheta_Y$  – coefficient in the relationship:  $\bar{p}_Y = \vartheta_Y Y$ ; according to von Mises yield criterion  $\vartheta_Y = 1.1$ ,
- $F$  – normal force,
- $P$  – external constant load,
- $F_Y$  – limiting normal force for elastic deformation,
- $\delta$  – total indentation (relative approach),
- $\delta_Y$  – limiting indentation for elastic deformation,
- $\delta_c$  – maximum indentation,
- $\delta_r$  – change in indentation during unloading,
- $\delta_f$  – final indentation, when the compressed bodies separate,  $\delta_f = \delta_c - \delta_r$ ,
- $R_*$  – effective radius of contact curvature,
- $\bar{R}_*$  – effective radius of contact curvature after plastic deformation, when  $\delta = \delta_c$ ,
- $E_*$  – effective Young's modulus,
- $y(t)$  – vertical position of the mass centre of the moving mass,
- $y_C(t)$  – vertical position of the point of the half-space lying outside the contact zone,
- $y_b(x)$  – rigid constraint, *i. e.* the vertical position of the center sphere rolling on the rigid irregular surface, under the assumption of constant contact between them.

## 1. Introduction

The object of modelling and simulation is dynamic unilateral contact of hard deformable bodies. The contact is referred to as unilateral because the bodies may

separate from each other. The term “hard” means that the bodies’ compliance is small, in consequence of which the area of contact is very small in comparison to their cross sections, even though the normal forces and local relative displacements, elastic or plastic, are very high.

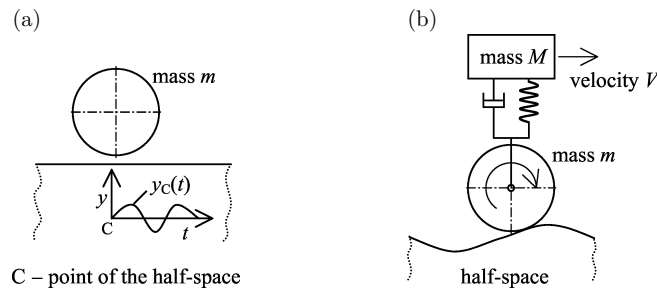


**Figure 1.** Examples of dynamic contact of hard compact bodies:  
 (a) sphere in contact with a half-space oscillating in a vertical plane;  
 (b) sphere rolling on the irregular surface of a half-space

Contact vibrations or vibro-impact motion may be excited for example by oscillations of one or both bodies (Figure 1a) or by surface irregularities (Figure 1b) in case of moving contact point. The word *moving* relates to internal coordinate systems fixed with the bodies. A moving contact point is present both in sliding and rolling motion.

The Hertz theory was developed 120 years ago and concerns the static contact of elastic smooth and non-conforming bodies. It provides a good basis for modelling and simulation of dynamic unilateral contact in case of loads (normal forces) which satisfy the assumptions of the theory, in particular the assumption that the strains within the contact zone are purely elastic and the material of the bodies is strain-rate independent.

The computer model was developed to widen the scope of the investigation for the cases in which the plastic region is present within the contact zone, but it is fully contained by the surrounding material which is still elastic. The computer model is based on analytical static models of hard bodies’ contact, *i.e.* the Hertzian model in elastic range [1, 2] and the Johnson’s model in elastic-plastic (*i.e.* contained plastic) range [3, 4]. In the Johnson’s model the relationship between the normal force and the relative approach (indentation) during unloading differs from that during loading, due to plastic deformations.

The development of an appropriate physical and computer model of dynamic unilateral contact of hard deformable bodies is important in the analysis of dynamical processes existing for instance in rolling bearings, cam mechanisms, gears and in train movement in the wheel/rail system [5].

## 2. Analytical Hertzian and Johnson’s model

In the strain and stress analysis in the contact zone of spherical bodies it is convenient to use the notions of effective modulus  $E_*$  and effective radius  $R_*$ . For two bodies of the radii  $R_1$ ,  $R_2$ , made of the material of the Young’s modulus  $E_1$ ,  $E_2$  and

the Poisson's numbers  $\lambda_1$ ,  $\lambda_2$  the effective modulus  $E_*$  and effective radius  $R_*$  are computed from the formulas:

$$1/R_* = (1/R_1 + 1/R_2) \quad 1/E_* = [(1 - \lambda_1^2)/E_1 + (1 - \lambda_2^2)/E_2]. \quad (1)$$

According to the Hertz theory, in the elastic range of deformations, the relationship between the normal force  $F$  and the indentation  $\delta$  during unloading is the same as during loading, and it is given by the formula:

$$F(\delta) = 4/3E_*R_*^{1/2}\delta^{3/2}. \quad (2)$$

On the basis of experimental observations some physical assumptions were made in the Johnson's model, and for these assumptions rigorous analytical relationships were obtained. During loading with the normal force greater than the limiting force  $F_Y$  (and less than  $F_p \approx 650F_Y$ ) the relationship  $F(\delta)$  is given by the formula:

$$F(\delta) = F_Y(2\delta/\delta_Y - 1)[1 + (3\vartheta_Y)^{-1} \ln(2\delta/\delta_Y - 1)]. \quad (3)$$

Even when plastic deformations occur during loading, unloading has entirely elastic character and therefore the relationship  $F(\delta)$  is analogous to (2):

$$F(\delta) = 4/3E_*\bar{R}_*^{1/2}(\delta - \delta_f)^{3/2}. \quad (4)$$

In formula (4) the symbol  $\bar{R}_*$  denotes a new value of the effective radius. In the Johnson's model the effective radius changes when  $\delta = \delta_c$ , *i.e.* when elastic-plastic loading ends, and elastic unloading starts. A new value is calculated by the formula  $\bar{R}_* = R_*(2\delta_c/\delta_Y - 1)^{1/2}$ . During unloading the indentation decreases from  $\delta_c$  to  $\delta_f$ , and the difference  $\delta_r = \delta_c - \delta_f$  equals  $\delta_r = \delta_Y(2\delta_c/\delta_Y - 1)^{1/2}$ .

Figure 2 shows the relationship  $F(\delta)$  in the range  $\langle 0, 4\delta_Y \rangle$  during loading and three force-indentation curves for three values of maximum indentation  $\delta_c$ , that is, for  $\delta_c = 2\delta_Y$ ,  $3\delta_Y$ ,  $4\delta_Y$ . The curve number 1 is a graph of relationship (2), *i.e.* it extrapolates the relevant Hertzian relationship beyond the range  $\langle 0, \delta_Y \rangle$ , in which purely elastic strains exist. Figure 3 represents the simplest model of elastic-plastic contact. In the elastic range the relationship  $F(\delta)$  is linear. External force  $F > F_Y$  induces plastic flow. The maximum indentation  $\delta_c$  and the final indentation  $\delta_f$  depend on the dynamics of the system and time history of external load. After changing the indentation scale into the relative strain scale and the normal force scale into the stress

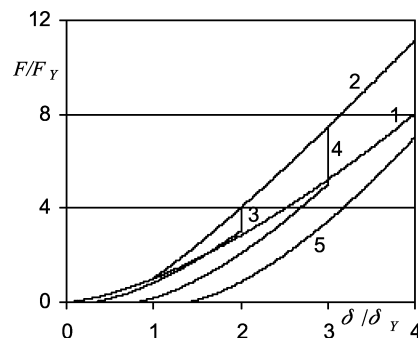


**Figure 2.** Force-indentation curves: 1 – by the Hertz theory, extrapolated for  $F > F_Y$ ; 2 – resulting from Johnson's model, during loading; 3, 4, 5 – resulting from Johnson's model, during unloading, for the maximum indentation  $\delta_c = 2\delta_Y$ ,  $3\delta_Y$ ,  $4\delta_Y$ , respectively

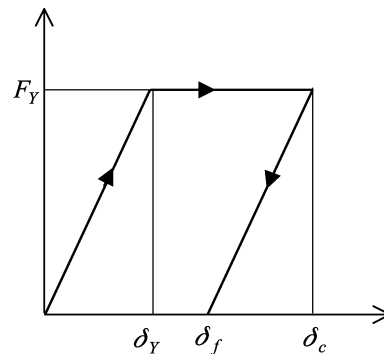


**Figure 3.** Force-indentation curve for linearly elastic and perfectly plastic model of contact

scale the graph in Figure 3 becomes the strain-stress characteristic of compression of elastic-purely plastic material. The Johnson's model of contact of spherical bodies assumes such a characteristic of material of both bodies in contact.

The occurrence of plastic deformations, their magnitude and area of plastic zone, depend very much on the uniaxial yield stress  $Y$ . According to the Hertz theory the limiting normal force  $F_Y$  for elastic deformations is determined by the formula:

$$F_Y = (3\pi/4)^2 \vartheta_Y Y R_*^2 (\vartheta_Y Y / E_*)^2. \quad (5)$$

For instance, for steel of compressive yield stress 1GPa the limiting force  $F_Y$  is as many as 1.95 times greater than for steel of yield stress 0.8GPa.

### 3. Investigation via computer simulation

Exemplary simulation results, shown in Figure 4, concern the case of oscillations of the mass  $m$  (see Figure 1a) lying at an initial time on the platform, which is a half-space in physical terms. At the initial instant of time the effective radius of one-point contact of the mass with the platform  $R_* = 0.475\text{m}$ . The mass is pressed with constant force  $P = 40\text{kN}$ , which is ten times greater than the weight of the oscillating mass  $m$ . The vertical motion of the platform, strictly speaking the motion of the points outside the contact zone which don't undergo displacements due to elastic and plastic deformations, is given by the harmonic: function  $z = -a + a \cos 2\pi f$ , the amplitude  $a = 0.1\text{mm}$ , and the frequency  $f = 560\text{Hz}$  is about two times greater than the contact resonance frequency. The excitation of such a frequency arises, for example, when the wheel of the rail vehicle rolls along a corrugated rail and the speed of the vehicle is 100km/h and the wavelength of corrugations is 5 cm.

At the present stage the mass-platform system is not yet a model of a specific technical system. The accepted values of parameters could be the parameters of a simplified model of contact between the wheel of a light rail vehicle and the rail. However, in the last case the contact is of moving (rolling) type, so for an appropriate relationship between oscillation frequency and rolling speed the contact zone moves with constant speed and within this moving zone only loading happens; force-indentation characteristic at unloading doesn't influence the vertical motion.

For comparison purposes Figure 5 presents three characteristic time patterns for entirely elastic vibro-impact system from Figure 1b. At low frequencies the bodies

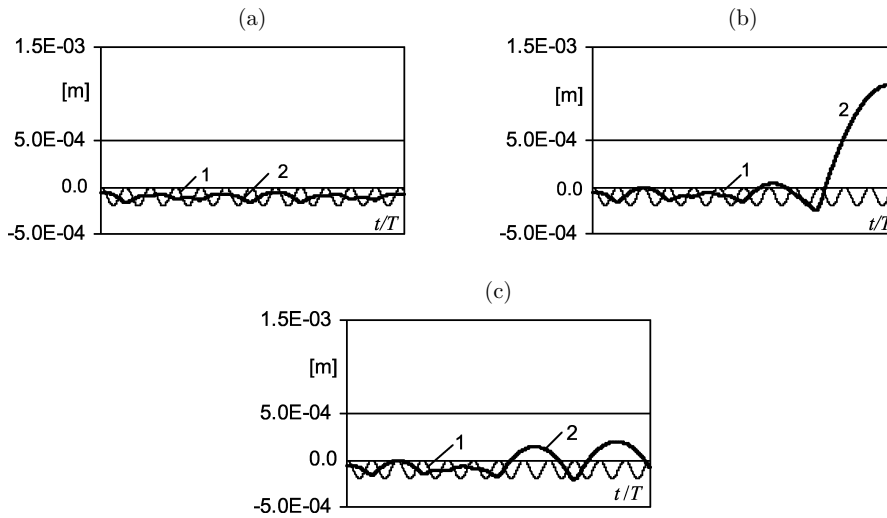


**Figure 4.** Simulation results for the system of Figure 1a with the Johnson's model of contact: (a) yield stress of the value  $Y = 10^9 \text{ N/m}^2$  is not exceeded, (b) non-moving contact point, yield stress  $Y = 6 \cdot 10^8 \text{ N/m}^2$  was exceeded; (c) moving contact point, yield stress  $Y = 6 \cdot 10^8 \text{ N/m}^2$  was exceeded. *Lines indications:* 1 – harmonic excitation  $y_C(t)$ , 2 – vertical position  $y(t)$  of the center of mass  $m$

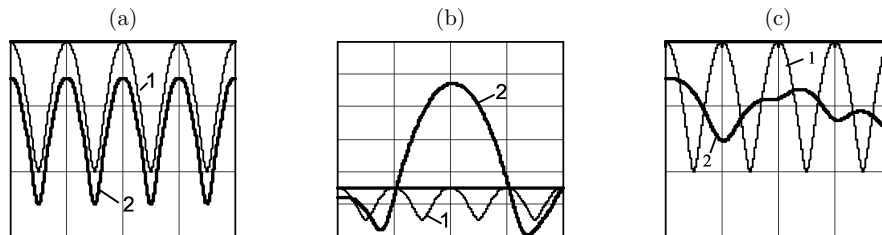


**Figure 5.** Three characteristic samples of time histories of the purely elastic system from Figure 1b for excitation frequency: (a) below the contact resonance frequency, (b) close to the resonance frequency, (c) over the resonance frequency. *Lines indications:* 1 – rigid constraint  $y_b(t)$ , 2 – sphere vertical position  $y(t)$

stay in contact. The difference between the rigid constraint  $y_b(t)$  and the mass centre vertical position  $y(t)$  is a measure of indentation  $\delta$ . When the bold line is over the thin one, the sphere and the platform do not contact each other. At frequencies close to the contact resonance frequency characteristic high bounces off the platform are observed, whereas at high frequencies the oscillation amplitude of the mass  $m$  is lesser than the amplitude of the rigid constraint and the bodies lose and come into contact alternately. The method for numerical computation of the rigid constraint  $y_b(t)$  for any given profile of irregular surface is presented in [5]. In the case of non-moving contact point and a smooth surface, like in the system of Figure 1a, the rigid constraint  $y_b(t)$  is equivalent to excitation  $y_C(t)$ .

Simulation results show that in the case of a non-moving contact point the dynamic behaviour of the system under investigation is determined to a large extent by a significant change of the effective radius  $R_*$  due to plastic deformation. In consequence of this change the contact stiffness increases, which appears for instance

in starting of bouncing of the mass after the first plastic deformation (see Figure 4b). Time history  $y(t)$  shown in Figure 4a, obtained for the same value of frequency of excitation as in Figure 4b, is characteristic for frequencies much higher than the contact resonance frequency, whereas high bouncing of the sphere off the platform shown in Figure 4b is typical at contact resonance. This situation can be explained as follows: the increase in contact stiffness moves the contact resonance frequency towards higher frequencies. Therefore the bouncing occurs at frequencies higher than in the case of high value of the yield stress  $Y$  (Figure 4a).

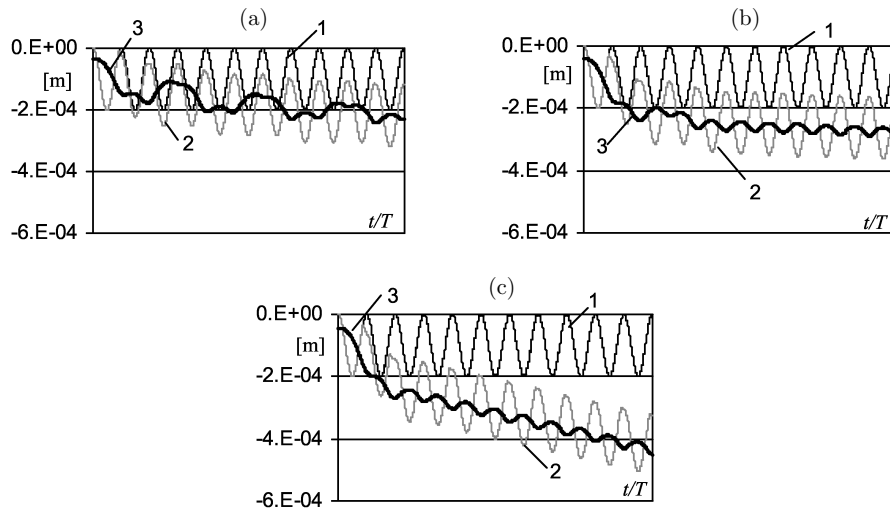


**Figure 6.** Simulation results for the system of Figure 1a, non-moving contact point, linearly elastic – perfectly plastic model of contact (see Figure 3), and for three different values of the external constant load  $P$ : (a) at the load  $P = 10 \cdot mg$ , (b) at the load  $P = 12 \cdot mg$ , (c) at the load  $P = 13 \cdot mg$ . Lines indications: 1 – harmonic excitation  $y_C(t)$ , 2 – change in a distance between two bodies' points being outside the contact region at the normal force  $F = 0\text{N}$ , so that the difference between the line 3 and the line 2 is the indentation  $\delta$ , 3 – vertical position of the mass center  $y(t)$  (moved downward by the value of radius  $R_*$ )

Figure 6 shows the results of simulation of the system from Figure 1a with a discrete model of compliance for the contact region; strictly speaking – the model consisting of a linear spring connected in series with a perfectly plastic element. The force-indentation characteristic is shown in Figure 3. The linear contact stiffness is equal to  $F_Y/\delta_Y$ . The limiting normal force  $F_Y$  and the limiting indentation  $\delta_Y$  were computed from the Hertzian formulas.

The system with the discrete contact model has entirely different dynamical properties from that with the continuum contact model by Johnson. Figure 6 shows three exemplary time histories. In the first case (Figure 6a) the limiting normal force for elastic deformation  $F_Y$  was exceeded only at the beginning of the oscillations, then the motion stabilises and the permanent deflection does not increase.

With an increase in constant load the amplitude of oscillations of the mass  $m$  decreases quickly with time, and simultaneously the two bodies approach each other quickly. Such a discrete elastic-perfectly plastic model seems to be more appropriate

for simulation of full plastic flow, which happens according to Johnson when the normal force is hundreds times greater than the limiting force  $F_Y$ .

Concluding, dynamic behaviour of the simple system under consideration with the contact model by Johnson is very complex, especially at frequencies near to the contact resonance frequency. In order to perform a more thorough and quantitative analysis sophisticated tools (software) and procedures for analysis of strongly non-linear dynamical systems are planned to be applied.

### **Acknowledgements**

The research included in this paper is partially supported by the Polish State Committee for Scientific Research under grant No 8 T12C 046 21.

### **References**

- [1] Harris T A 1966 *Rolling Bearing Analysis*, Wiley
- [2] Timoshenko S and Goodier J N 1951 *Theory of Elasticity*, McGraw-Hill
- [3] Johnson K L 1985 *Contact mechanics*, Cambridge University Press
- [4] Stronge W J 2000 *Impact Mechanics*, Cambridge University Press
- [5] Bogacz R and Kowalska Z 2001 *European Journal of Mechanics A/Solids* **20** 673

